JOURNAL OF GEOPHYSICAL RESEARCH, VOL. 101, NO. D12, PAGES 16,973–16,985, JULY 27, 1996

Sensitivity of cirrus cloud albedo, bidirectional reflectance and optical thickness retrieval accuracy to ice particle shape

Michael I. Mishchenko,[1] William B. Rossow,[2] Andreas Macke,[3] and Andrew. A. Lacis[2]

Abstract. We examine the sensitivity of cirrus cloud albedo and bidirectional reflection function to particle shape using the phase functions of liquid water spheres, regular hexagonal ice crystals, and random-fractal ice particles calculated at a nonabsorbing visible wavelength of 0.63 μm. Accurate multiple-scattering calculations for plane-parallel clouds show that hexagonal ice crystal clouds have systematically larger planetary and global albedos than liquid water clouds of the same optical thickness. There is accumulating evidence that the idealized phase function of regular hexagonal crystals, which causes pronounced halos, is not necessarily the best representation of the range of reflectance characteristics of the majority of ice clouds. A more typical representation of the scattering phase function for ice clouds that are composed of a complex set of crystal shapes and sizes may be obtained using a model of randomly shaped irregular particles. Even larger cloud albedos are obtained for the random-fractal particle model because of its smaller asymmetry parameter. Our computations also show that a larger planetary albedo does not always imply a larger reflectance and that the relative brightness of ice versus liquid water clouds is highly scattering-geometry dependent. Use of the wrong particle shape model (crystal instead of water droplet and vice versa) in retrieving cloud optical thickness from bidirectional reflectance measurements can result in an underestimation or overestimation of the true optical thickness by a factor that can exceed 3. At some scattering geometries, use of the wrong model can give an unrealistically large optical thickness or no solution at all. Overall, bidirectional reflectance differences between random-fractal and regular hexagonal particle shapes are significantly smaller than those between either ice crystal and liquid water spheres, except at the back scattering direction.

1. Introduction

Many experimental and theoretical studies suggest that the single-scattering properties of nonspherical ice cloud particles can differ substantially from those of surface- or volume-equivalent spheres [e.g., *Sassen and Liou*, 1979; *Volokovitskiy et al.*, 1980; *Takano and Liou*, 1989; *Macke*, 1993; *Zhang and Xu*, 1995; *Iaquinta et al.*, 1995, and references therein]. The single-scattering differences, in turn, affect the bidirectional reflection function and therefore the accuracy of optical thickness retrievals for ice clouds from remote sensing measurements, particularly from satellites [*Kinne and Liou*, 1989; *Minnis et al.*, 1993a]. Moreover, these differences affect the relationship between ice cloud microphysical properties and cloud albedo and, consequently, the fidelity of climate model representations of cloud radiative feedbacks. The most common ice particle shape used in theoretical analyses is the regular hexagonal crystal [*Takano and Liou*, 1989; *Kinne and Liou*, 1989; *Minnis et al.*, 1993a,b; *Fu and Liou*, 1993; *Sun and Shine*, 1995]. However, there is accumulating evidence that the idealized phase function of regular hexagonal particles is not representative of the reflectance characteristics of the majority of cirrus clouds.

Regular hexagonal crystals, either single or aggregated, produce strong halo features in the angular distribution of reflected sunlight [*Takano and Liou*, 1989; *Macke*, 1993] that are rarely observed in practice. In particular, recent ground-based, in situ nephelometer, and aircraft radiance measurements of cirrus clouds [*Foot*, 1988; *Francis*, 1995; *Gayet et al.*, 1995; *Posse and von Hoyningen-Huene*, 1995] show that ice cloud scattering phase functions can be rather featureless with no appreciable halos. *Sassen et al.* [1994], *Macke* [1994], and *Macke et al.* [1996] show that the necessary condition for halo production is perfect regularity of the particle shape, whereas real cirrus clouds are typically composed of particles with very complicated, highly irregular shapes [*Sassen et al.*, 1994; *Arnott et al.*, 1994; *Francis*, 1995]. Thus the particle growth processes in most cirrus

[1]NASA Goddard Institute for Space Studies, New York, and Institute of Terrestrial and Planetary Atmospheres, State University of New York at Stony Brook.

[2]NASA Goddard Institute for Space Studies, New York.

[3]Columbia University and NASA Goddard Institute for Space Studies, New York.

Copyright 1996 by the American Geophysical Union.

Paper number 96JD01155.
0148-0227/96/96JD-01155$9.00

clouds may result in crystal habits (shapes) that are unsuitable for halo formation [*Wielicki et al.*, 1990; *Minnis et al.*, 1993b].

More recent ray-tracing computations by *Macke et al.* [1996] suggest that to suppress the halo features of regular hexagonal crystals, the ice particle shape should possess a certain degree of irregularity and, more importantly, randomness. *Macke et al.* [1996] model ice particles by considering both random fractals and hexagonal columns/plates with imposed random facet tilts. They find that the magnitude of the halo features decreases rapidly with increasing distortion parameter, making them essentially unobservable.

Minnis et al. [1993a] examined the impact of using the scattering phase function of hexagonal ice crystals instead of the phase function of liquid water droplets (spheres) used by the International Satellite Cloud Climatology Project (ISCCP) [*Rossow and Schiffer*, 1991; *Rossow et al.*, 1996] to analyze satellite-measured radiances from cirrus clouds. A companion paper [*Minnis et al.*, 1993b] shows that using a radiative retrieval model based on the regular hexagonal shape significantly improves the determination of the properties of optically thin cirrus; however, the effects for optically thicker ice clouds were not considered. The unique single-scattering properties of randomly shaped ice particles suggest a complimentary theoretical investigation of the potential effect of random particle shape on cloud albedo and bidirectional reflectance. Specifically, in this paper we compare visible cloud albedos and bidirectional reflectances computed using the scattering phase functions of random-fractal ice particles, regular-hexagonal crystals, and liquid water spheres. In the following section we briefly discuss numerical aspects of single- and multiple-scattering computations and report results of detailed albedo and bidirectional reflectance calculations at a nonabsorbing visible wavelength of $\lambda = 0.63$ μm. We consider a range of optical thicknesses from 0.01, the single-scattering regime, to 300, effectively the asymptotic limit. These calculations are then analyzed to ascertain the errors in retrieved cloud optical thickness and albedo caused by using different cloud particle shape assumptions.

2. Computations

To model scattering properties of irregularly shaped ice particles, we use a randomized version of the second generation triadic Koch fractal [*Macke*, 1994; *Macke et al.*, 1996]. This particle is shown in Figure 1 and is obtained by introducing random displacements of the tetrahedrons forming the second generation regular Koch fractal. The distortion parameter is defined as the ratio of the maximum displacement to the length of the tetrahedron segment and was increased until the phase function of the fractal in random orientation converged and became insensitive to further increasing distortion. In other words, for distortion parameters above some critical value the fractal phase function becomes invariant against particular realizations of the random particle shape and thus may represent the middle of the range of phase functions of highly irregular natural ice crystals.

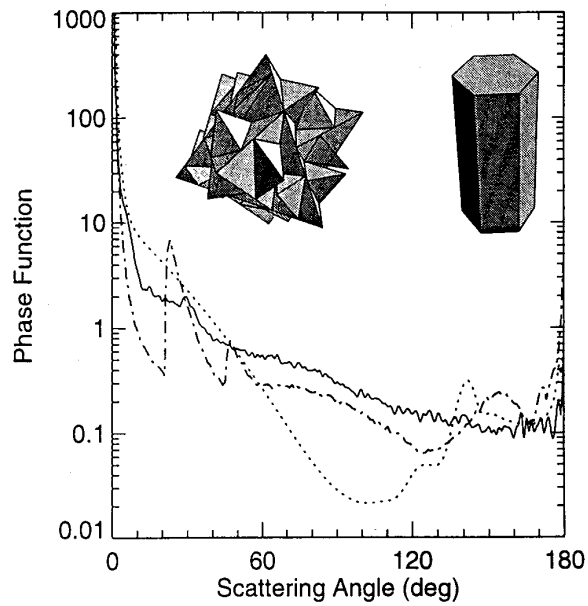

Figure 1. Single-scattering phase functions versus scattering angle for randomly oriented, random-fractal ice particles (solid curve), randomly oriented hexagonal columns with length-to-diameter ratio 2 (dotted-dashed curve), and International Satellite Cloud Climatology Project (ISCCP) liquid water droplets (dotted curve) at $\lambda = 0.63$ μm. The insert depicts the random-fractal and the regular hexagonal particles studied in this paper.

The scattering component of the random-fractal phase function was computed using the standard ray-tracing technique, as described by *Macke et al.* [1996] and *Muinonen et al.* [1989]. Since water ice is almost nonabsorbing at visible wavelengths [*Warren*, 1984], this scattering component is essentially size independent. The size-dependent diffraction component of the phase function at $\lambda = 0.63$ μm was averaged over a power law distribution of particle sizes with effective radius $r_{\mathrm{eff}} = 30$ μm and effective variance $v_{\mathrm{eff}} = 0.1$. The cross-section-weighted effective mean radius and the effective variance of a size distribution are defined as [*Hansen and Travis*, 1974]

$$r_{\mathrm{eff}} = \frac{1}{G} \int_0^\infty r \pi r^2 n(r)\, dr, \tag{1}$$

$$v_{\mathrm{eff}} = \frac{1}{G r_{\mathrm{eff}}^2} \int_0^\infty \left(r - r_{\mathrm{eff}}\right)^2 \pi r^2 n(r)\, dr, \tag{2}$$

where $n(r)dr$ is the fraction of particles with (equivalent sphere) radii from r to $r + dr$, and

$$G = \int_0^\infty \pi r^2 n(r)\, dr \tag{3}$$

is the average particle geometric cross-sectional area. In

many cases, cirrus cloud particles can have larger effective radii. However, since these particles are nonabsorbing and already much larger than the wavelength, further increase of the effective radius would only change the value of the phase function at exactly the forward scattering direction leaving the rest of the phase function and the asymmetry parameter intact. In contrast, reflectance at absorbing wavelengths would be much more sensitive to the particle size [*Mitchell and Arnott*, 1994].

The resulting phase function computed at the wavelength $\lambda = 0.63$ μm is shown in Figure 1 by the solid curve. For comparison, the dotted-dashed curve shows the phase function computed for projected-area-equivalent, randomly oriented hexagonal columns with length-to-diameter ratio 2 and the same effective radius $r_{\mathrm{eff}} = 30$ μm, whereas the dotted curve shows the phase function for the liquid water sphere model (gamma distribution of spherical droplets with an effective radius $r_{\mathrm{eff}} = 10$ μm and effective variance $v_{\mathrm{eff}} = 0.1$) used in the ISCCP [*Rossow and Schiffer*, 1991; *Rossow et al.*, 1996]. The fractal phase function is relatively featureless, shows no deep and wide side-scattering minimum and no strong rainbow characteristic of liquid water droplets [*Hansen and Travis*, 1974], and reveals no pronounced halos typical of regular hexagonal particles [*Takano and Liou*, 1989; *Macke*, 1993]. This weak scattering-angle dependence of the fractal phase function at side-scattering and backscattering angles is in qualitative agreement with laboratory and in situ measurements of real ice crystals [*Sassen and Liou*, 1979; *Volkovitskiy et al.*, 1980; *Foot*, 1988; *Francis*, 1995; *Gayet et al.*, 1995; *Posse and von Hoyningen-Huene*, 1995]. Figure 1 demonstrates that differences between the ice particle phase functions and the water droplet phase function are large and that the fractal-particle to water droplet phase function ratio can exceed 10 at side-scattering angles. Such large single-scattering differences may not necessarily be eliminated by multiple scattering in clouds, which makes their effect on cloud albedo and bidirectional reflectance worth studying [cf. *Minnis et al.*, 1993a].

Importantly, the random-fractal phase function shown in Figure 1 essentially coincides with the phase function computed by J. Peltoniemi (private communication, 1995) for a stochastically rough nonspherical ice particle with a sufficiently large standard deviation of surface radius and slope. The process of generating a stochastically rough nonspherical particle and the ray-tracing technique used are described by *Peltoniemi et al.* [1989]. The excellent quantitative agreement between the phase functions obtained using two quite different generators of a totally random nonspherical particle may suggest that these phase functions indeed capture the scattering character of highly variable and irregular natural ice crystals. Indeed, although each individual ice particle at a given time and place has a specific, albeit irregular shape, cirrus clouds are commonly observed to exhibit large time and space variations of particle shapes. All practical treatments, remote sensing or modeling, of radiation consider only average properties over finite space and time scales. For example, satellite radiance measurements represent an average over scales ~1-10 km typically. Therefore such average cirrus clouds should be thought of as mixtures of a wide variety of irregular particle shapes whose average scattering properties can well be represented by a single randomly shaped particle.

We have used the three phase functions shown in Figure 1 in accurate radiative transfer calculations for plane-parallel ice and water clouds with varying optical thickness τ. We found that because of the large particle size in comparison with the wavelength, the multiple-scattering computations were demanding and required special precautions in order to ensure the desired accuracy. Since the ray-tracing part of the ice particle phase functions was initially computed for 181 equidistant scattering angles, we first used spline interpolation to recompute it for division points of a high-order Gaussian quadrature formula and then added the analytically computed diffraction component to obtain the total phase function $P(\Theta)$, where Θ is the scattering angle. The total phase function values computed at the Gaussian division points were used to calculate via the formula

$$\omega_n = \frac{2n+1}{2} \int_{-1}^{1} d(\cos\Theta)\ P(\Theta)\ P_n(\cos\Theta) \qquad (4)$$

the expansion coefficients ω_n appearing in the standard expansion of the phase function in Legendre polynomials $P_n(\cos\Theta)$ [*van de Hulst*, 1980]:

$$P(\Theta) = \sum_{n=0}^{n_{\max}} \omega_n\ P_n(\cos\Theta). \qquad (5)$$

The expansion coefficients ω_n for the water droplet phase function were computed using Mie theory and the method described by *de Rooij* [1984]. We found that the expansion of equation (5) required many terms in order to accurately reproduce the original phase function. Specifically, the length $n_{\max}$ of the expansion was 1000 for the ice particle phase functions and 600 for the water droplet model.

The expansion coefficients were then used to compute the Fourier components of the phase function appearing in the Fourier decomposition of the radiative transfer equation. Finally, the bidirectional cloud reflectance for cloud optical thickness varying from 0.01 to 300 was computed using the doubling and invariant imbedding methods [*Lacis and Hansen*, 1974; *van de Hulst*, 1980; *Sato et al.*, 1977; *Mishchenko*, 1990] without introducing any approximations like the truncation of the forward scattering peak of the phase function. The underlying surface was assumed to be totally absorbing and Rayleigh scattering in the atmosphere was ignored. The number of Gaussian quadrature points N_G in the zenith angle discretization and the number of terms N_F in the azimuthal Fourier decomposition of the reflection function R were increased until the relative accuracy of computing R was better than 10^{-3}. Specifically, we used $N_G = 290$ for both water and ice clouds, while the convergent value of the parameter N_F was 200 for water clouds and 300 for ice clouds. Although the relative accuracy of 10^{-3} for computed reflectances may seem to be excessively high for most practical applications, it ensures that our discussion and conclusions, especially those for optically very thick clouds,

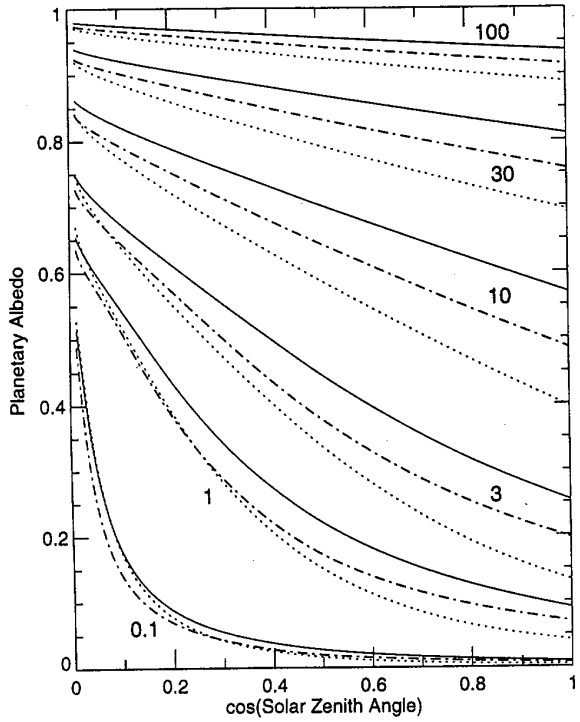

Figure 2. Planetary albedo versus cosine of the solar zenith angle for a plane-parallel cloud composed of randomly oriented fractal ice particles (solid curves), randomly oriented hexagonal columns (dotted-dashed curves), and ISCCP liquid water droplets (dotted curves). The labels show the values of the cloud optical thickness.

are not affected by purely numerical artifacts. Note that the higher-order Fourier components of the reflection function converge with increasing cloud optical thickness (much) faster than the lower-order components [*Sato et al.*, 1977]. For example, for all three particle models the Fourier components with $n \geq 1$ converged before cloud optical thickness reached 10 and did not change with increasing τ, so that only the zeroth component needed to be computed for $\tau \geq 10$. Therefore the explicit use of this behavior in the computer code allowed us to drastically speed up the multiple-scattering calculations. To ensure energy conservation and to further improve the computational accuracy, we have used the renormalization of the zeroth Fourier component of the phase function and the separation of the first-order-scattering contribution to the reflection function as described by *Hansen* [1971], *Wiscombe* [1976], and *de Haan et al.* [1987].

The main results of our extensive computations are summarized in Figures 2 and 3 and Plates 1-4. Figure 2 shows the planetary (local) albedo A_p as a function of cosine of the solar zenith angle μ_0 for six values of the cloud optical thickness τ = 0.1, 1, 3, 10, 30, and 100. The planetary albedo is defined as [*van de Hulst*, 1980]

$$A_p(\mu_0) = \frac{1}{\pi}\int_0^{2\pi} d\phi \int_0^1 d\mu\,\mu R(\mu,\mu_0,\phi) = 2\int_0^1 d\mu\,\mu R^0(\mu,\mu_0), \tag{6}$$

where μ is cosine of the zenith angle of the reflected light, ϕ is the relative azimuth angle between the meridian planes of the reflected and incident light, and R^0 is the zeroth (azimuth independent) Fourier component of the reflection function. Figure 3 demonstrates the optical thickness dependence of the spherical (global) albedo defined by [*van de Hulst*, 1980]

$$A_s = 2\int_0^1 d\mu_0\mu_0 A_p(\mu_0). \tag{7}$$

Plate 1 shows the ratio $R_f(\tau)/R_w(\tau)$ of the fractal-particle ice cloud to the liquid water cloud reflection functions as a function of μ and μ_0 for cloud optical thicknesses τ = 0.3, 1, 3, 30, and 300 and relative azimuth angles ϕ = 0° (forward scattering azimuth), 60° and 120° (side-scattering azimuths), and 180° (backscattering azimuth). Analogously, Plate 2 shows the ratio $R_f(\tau)/R_h(\tau)$ of the fractal-particle to hexagonal-particle cloud reflection functions for the same optical thicknesses. In Plate 3 we show the ratio $R_f(\tau_f)/R_w(\tau_w)$ with water cloud optical thickness τ_w fixed at 3 and fractal-particle ice cloud optical thickness τ_f varying from 0.3 to 300. Similarly, Plate 4 shows the ratio $R_w(\tau_w)/R_f(\tau_f)$ for τ_f fixed at 1 and τ_w varying from 0.3 to 30. Note that because of the reciprocity relation [*van de Hulst*, 1980]

$$R(\mu_0,\mu,\phi) = R(\mu,\mu_0,\phi), \tag{8}$$

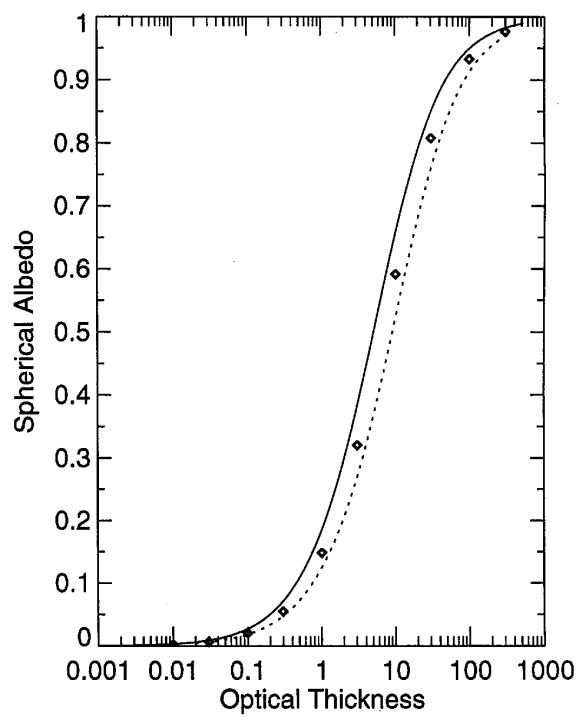

Figure 3. Spherical albedo versus optical thickness for a plane-parallel cloud composed of randomly oriented fractal ice particles (solid curve), randomly oriented hexagonal columns (diamonds), and ISCCP liquid water droplets (dotted curve).

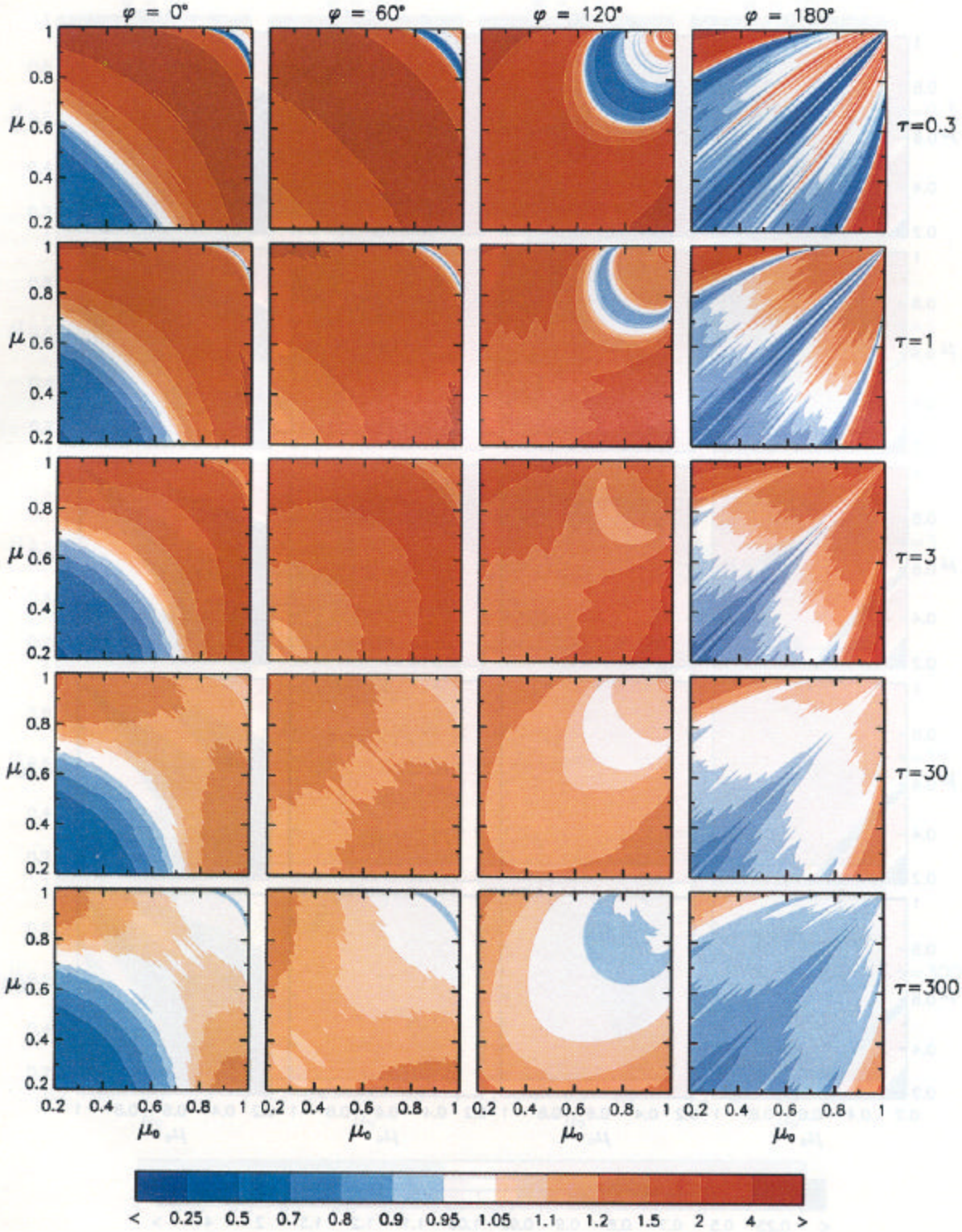

Plate 1. Ratio $R_f(\tau)/R_w(\tau)$ of the fractal-particle ice cloud to the liquid water cloud reflection functions versus μ, μ_0, and ϕ for cloud optical thickness τ varying from 0.3 to 300.

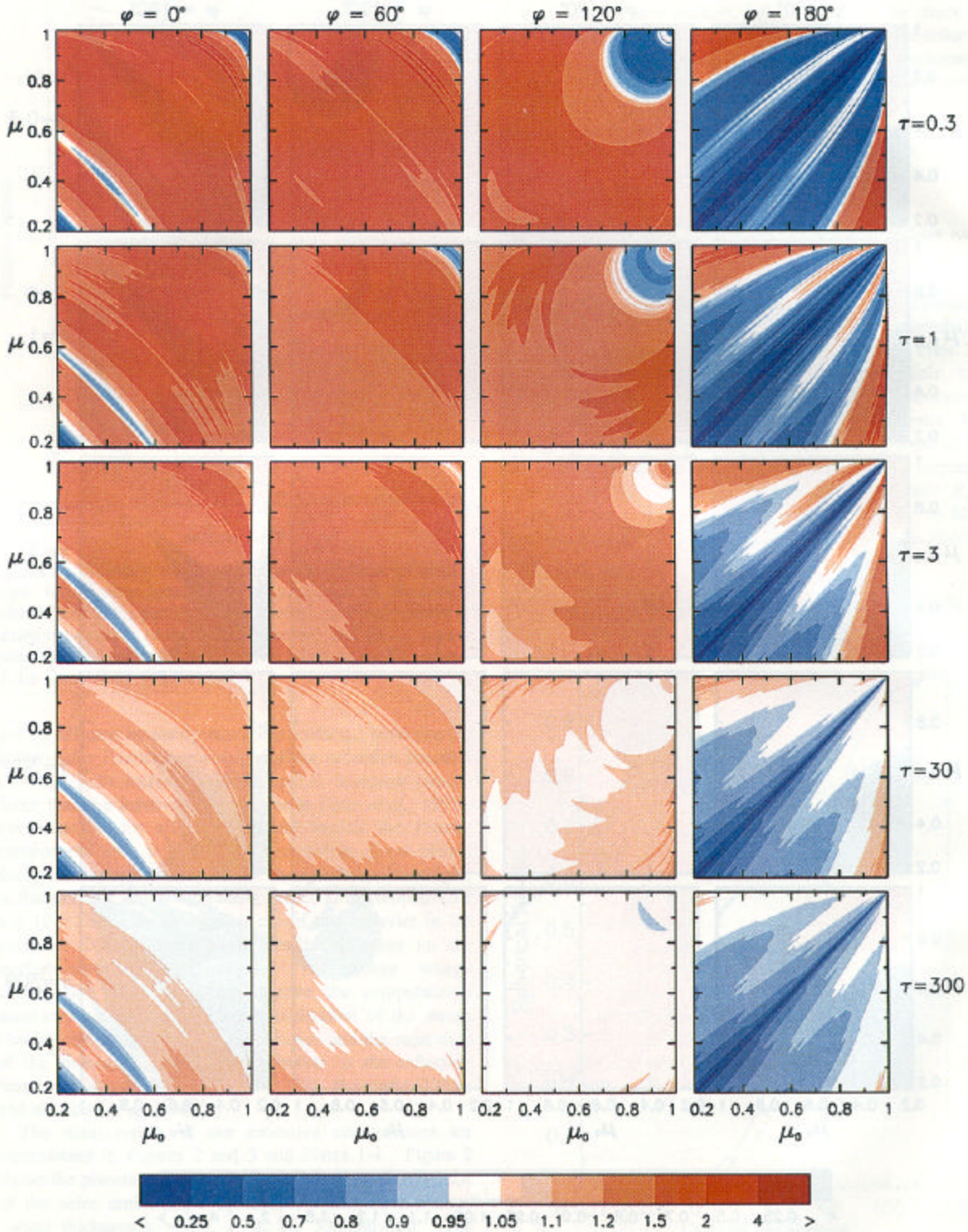

Plate 2. Ratio $R_f(\tau)/R_h(\tau)$ of the fractal-particle ice cloud to the hexagonal-crystal ice cloud reflection functions versus μ, μ_0, and ϕ for cloud optical thickness τ varying from 0.3 to 300.

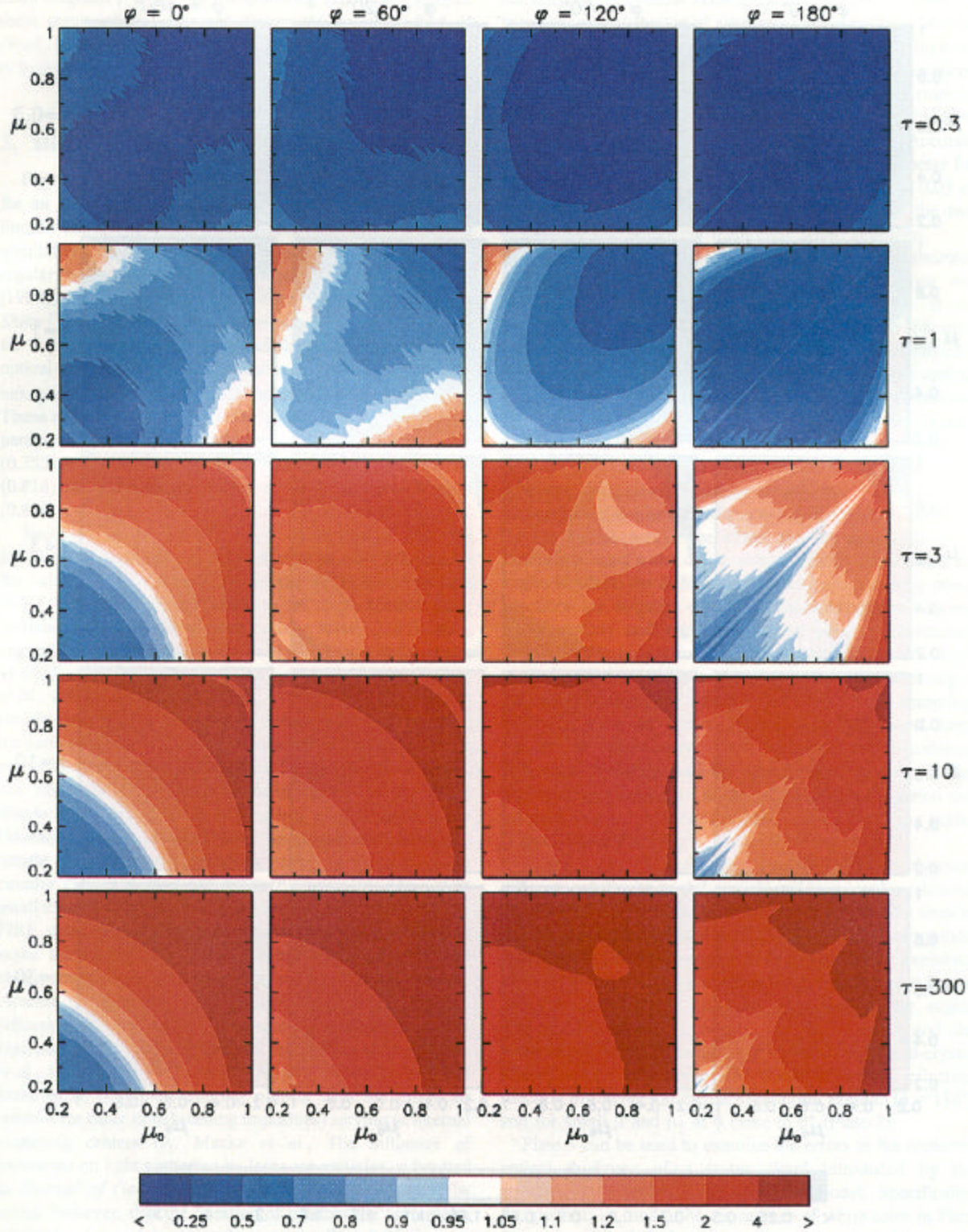

Plate 3. Ratio $R_f(\tau_f)/R_w(\tau_w)$ of the fractal-particle ice cloud to the liquid water cloud reflection functions versus μ, μ_0, and ϕ for water cloud optical thickness τ_w fixed at 3 and ice cloud optical thickness τ_f varying from 0.3 to 300.

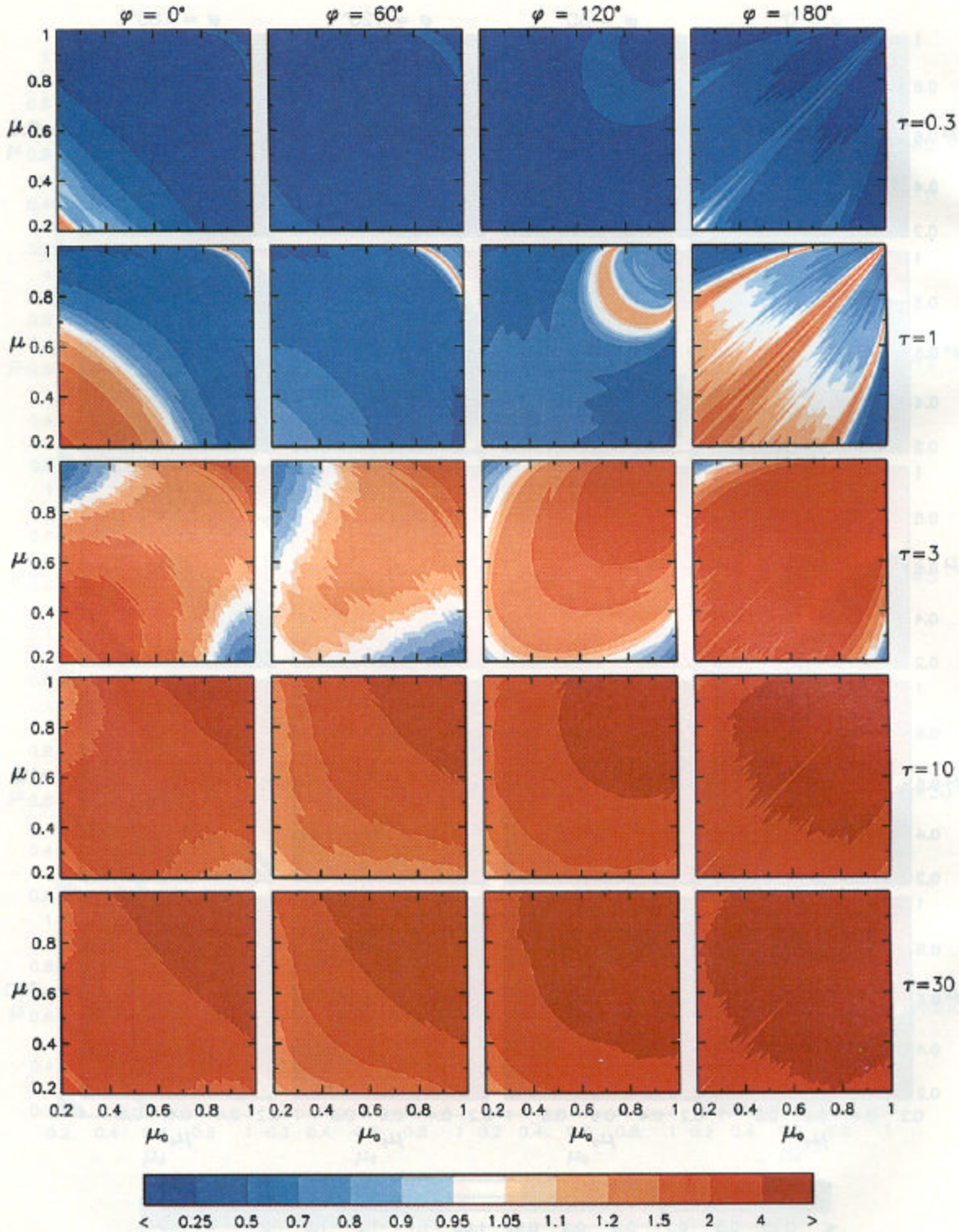

Plate 4. Ratio $R_w(\tau_w)/R_f(\tau_f)$ of the liquid water cloud to the fractal-particle ice cloud reflection functions versus μ, μ_0, and ϕ for ice cloud optical thickness τ_f fixed at 1 and water cloud optical thickness τ_w varying from 1 to 30.

all diagrams in Plates 1-4 are symmetrical with respect to the main diagonal $\mu = \mu_0$. In the following section we analyze these computational data and discuss the possible effect of cloud particle shape on cloud albedo and bidirectional reflectance.

3. Discussion

Figures 2 and 3 show that the planetary and global albedos for an ice cloud are systematically larger than those for a liquid water cloud *of the same optical thickness*, which is in qualitative agreement with analogous computations for regular hexagonal crystals reported by *Kinne and Liou* [1989], *Minnis et al.* [1993a], *Macke* [1994], and *Sun and Shine* [1995]. Furthermore, the planetary and global albedos for a fractal-particle ice cloud are larger than those for an optical-thickness-equivalent ice cloud composed of regular hexagonal particles, especially at optical thicknesses $\lesssim 10$. These results can be explained by the fact that the asymmetry parameter of the phase function for fractal ice particles (0.752) is smaller than that for regular hexagonal ice particles (0.816) and much smaller than that for liquid water droplets (0.862).

Stephens et al. [1990] have demonstrated that the influence of cirrus clouds on climate is strongly affected by the value of the asymmetry parameter of the cloud particle phase function. Some analyses of experimental data, including First ISCCP Regional Experiment (FIRE) data, suggest asymmetry parameter values for cirrus cloud particles as small as 0.75 or even less [*Stephens et al.*, 1990; *Wielicki et al.*, 1990; *Kinne et al.*, 1992, 1994]. If these estimates are correct, then our calculations demonstrate that modeling ice particle scattering properties in terms of the liquid droplet model and even using the standard hexagonal-crystal model can result in a significant underestimation of the cloud albedo. Importantly, as ray-tracing computations show [*Macke and Mishchenko*, 1996], no simple particle shapes (single or aggregated hexagons, cubes, spheroids, finite circular cylinders, etc.) can produce asymmetry parameters small enough to agree with the abovementioned results of the FIRE data analyses. It thus appears that the only way to make the ice particle phase function more isotropic and obtain small asymmetry parameter values is to considerably increase the contribution of multiple internal and external reflections by assuming a high degree of randomness and/or macroscopic surface roughness of the particle shape [*Macke et al.*, 1996; *Muinonen et al.*, 1996] or to model cirrus cloud particles as multiple-scattering objects with numerous air bubbles (or other nonabsorbing impurities) serving as internal scattering centers (A. Macke *et al.*, The influence of inclusions on light scattering by large ice particles, submitted to *Journal of Geophysical Research*, 1995). It should be noted, however, that the question of whether the asymmetry parameter for real ice crystals is as small as 0.75 or even smaller remains controversial, and further experimental and theoretical research in this area is definitely required [cf. *Stackhouse and Stephens*, 1991; *Francis et al.*, 1994]. If it turns out that the asymmetry parameter for real ice cloud particles is of the order of 0.8 or larger and the phase function is still relatively featureless and has no halos, then the only way to model such phase function is to assume a broad shape distribution of relatively simple particles lacking the perfect hexagonal structure [e.g., *Bohren and Singham*, 1991, and M. I. Mishchenko *et al.*, Modeling phase functions for dust-like tropospheric aerosols using a shape mixture of randomly oriented polydisperse spheroids, submitted to *Journal of Geophysical Research*, 1996]. Accurate experimental measurements of the asymmetry parameter for real cirrus cloud particles (accuracy of the order of 0.03 or better) would be useful in discriminating between the two mechanisms of producing featureless phase functions.

Comparison of Figures 2 and 3 and Plate 1 demonstrates that a larger spherical or planetary albedo does not necessarily imply larger bidirectional reflectance at all scattering geometries. Despite their (much) smaller spherical and planetary albedos, water clouds can be substantially brighter than fractal-particle ice clouds of the same optical thickness, especially at forward and backscattering directions. Somewhat unexpectedly, Plate 1 reveals a rather complicated structure demonstrating that nonspherical-spherical differences in bidirectional reflectance are strongly scattering-geometry dependent. Comparison of Plate 1 and Figure 4 shows that maximum differences between reflection functions for the fractal-particle ice cloud and the optical-thickness equivalent liquid water cloud occur at exactly those scattering angles at which the differences in the single-scattering phase functions are largest. Similar differences appear between fractal-particle and regular-hexagonal particle reflectances (Plate 2). The bidirectional reflectance differences are larger at smaller optical thicknesses and decrease with increasing τ, thus demonstrating the blurring effect of multiple scattering. However, even an optical thickness of 300 is not large enough to completely wash out the single-scattering differences resulting from the pronounced rainbow and deep side-scattering minimum in the spherical phase function and stronger spherical scattering at near-forward scattering angles (Figure 1 and Plate 1).

Plates 1 and 2 show that overall reflection function differences between fractal-particle and hexagonal-particle ice clouds of the same optical thickness are significantly smaller than those between fractal-particle and liquid water clouds, especially at side-scattering azimuths. This can be explained by much smaller single-scattering differences between fractal and hexagonal phase functions at side-scattering angles (Figures 1 and 4). However, the strong halos and the pronounced backscattering peak in the hexagonal-crystal phase function cause appreciable fractal-hexagonal reflection function differences at the backscattering azimuth ($\phi = 180°$) and for small μ and μ_0 at ϕ close to 0° (Plate 2).

Plate 3 can be used to examine the errors in the retrieved optical thickness of a water cloud introduced by the erroneous use of the fractal-particle ice model. Specifically, for given μ, μ_0, and ϕ the appearance of white color in Plate 3 at some optical thickness τ_f indicates that the brightness of the ice cloud with the optical thickness τ_f matches the brightness of the water cloud with the optical thickness $\tau_w = 3$. Similarly, Plate 4 can be used to estimate the error in the retrieved optical thickness of a fractal-particle ice cloud induced by the erroneous use of the liquid water droplet

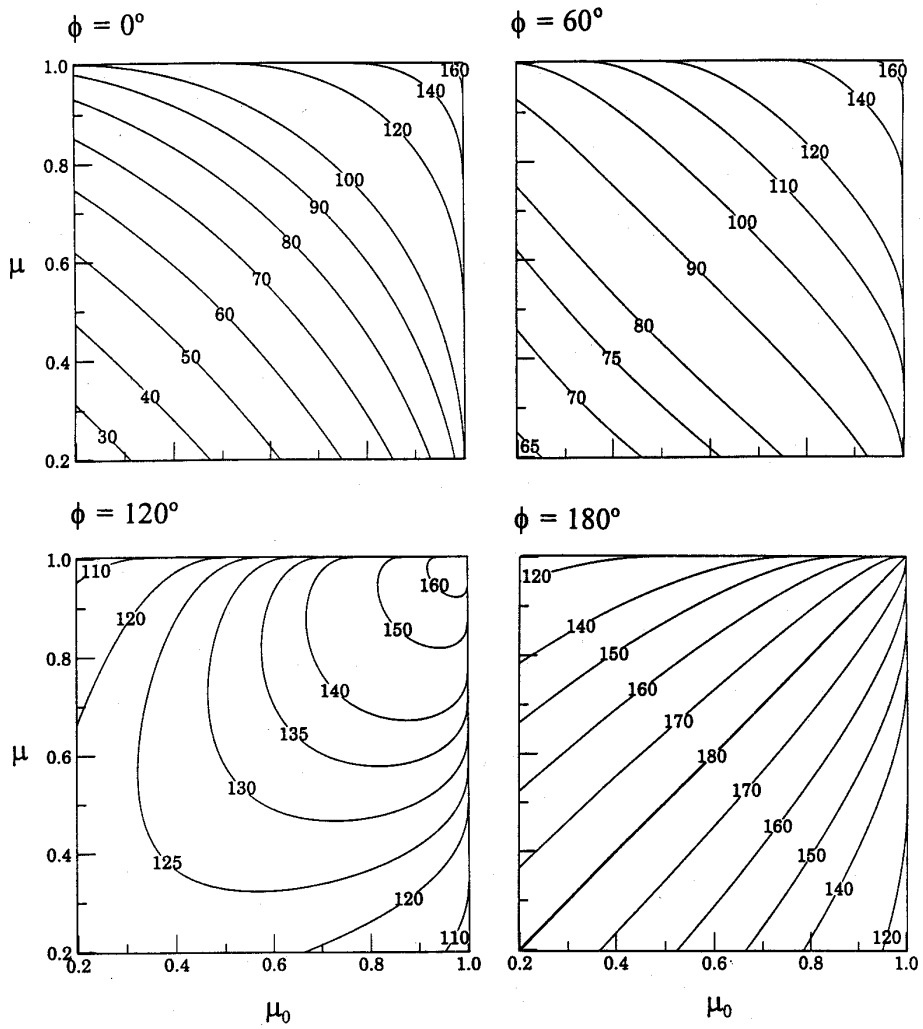

Figure 4. Scattering angle versus μ and μ_0 for ϕ = 0°, 60°, 120°, and 180°.

model. It is seen from Plates 3 and 4 that the retrieved optical thickness is strongly scattering-geometry dependent and can differ from the actual value by a factor that can exceed 3 [cf. *Mishchenko et al.*, 1995]. Following the differences in the single-scattering phase functions (Figure 1), the fractal-particle ice cloud model overestimates the retrieved optical thickness at near-forward and backscattering geometries, especially at small μ and μ_0, and underestimates it at side-scattering geometries (Plate 3 and Figure 4). The opposite is true if the liquid-droplet model is used to analyze reflectance measurements of an ice cloud (Plate 4). At most scattering geometries the erroneous use of the water droplet model results in an overestimation of the optical thickness of a fractal-particle ice cloud. Our computations (not shown here) also demonstrate that this holds for an ice cloud composed of the regular hexagonal crystals, in agreement with the conclusion of *Minnis et al.* [1993a].

The errors in the retrieved optical thickness of a water cloud resulting from the use of the fractal-particle model are especially large at near-forward scattering geometries, i.e., at ϕ close to 0° and small μ and μ_0. Remarkably, at ϕ = 0° and μ and μ_0 smaller than about 0.6, the reflectivity of the water cloud with τ_w = 3 cannot be reproduced by the ice cloud with optical thickness as large as 300 (Plate 3). Our computations show that the blue region at ϕ = 0° and small μ and μ_0 in Plate 3 survives even if the ice cloud becomes semi-infinite. This means that at near-forward scattering geometries water clouds with optical thickness of the order of 3 can produce reflectivities that cannot be matched by an ice cloud with an arbitrarily large optical thickness. Therefore at ϕ close to 0° and small μ and μ_0 the retrieval scheme using the fractal-particle ice model produces no solution at all. Importantly, our computations (not shown here) also suggest that this conclusion holds for hexagonal ice particles as well with the exception of the region of μ and μ_0 smaller than 0.25 where the strong primary halo in the hexagonal phase function reverses the situation.

The effect of using the wrong model to retrieve the cloud optical thickness and then to compute the cloud global albedo

can be twofold. As Plate 4 suggests, for most side-scattering geometries applying the liquid water model to analyze reflectance of a fractal-particle ice cloud results in an overestimation of the optical thickness. However, the global albedo of a liquid water cloud is always smaller than that of an optical-thickness-equivalent ice cloud (Figure 3). Therefore if the same liquid water model is consistently used in the optical thickness retrieval and albedo calculation, the errors are expected to partly cancel out (see Figure 3). The same cancellation of errors is expected if the ice particle model is used to analyze side-scattering reflectance measurements of a liquid water cloud (Plate 3). On the other hand, in both cases the errors will escalate rather than cancel out if reflectance data are obtained at forward or backscattering geometries (compare Plates 3 and 4 and Figure 4). An important practical case is the reanalysis of the ISCCP data replacing the water droplet model by the fractal ice crystal model for colder clouds. The average cloud optical thickness can be expected to decrease, but whether the resulting spherical albedo is higher or lower than previously calculated will depend on the distribution of cloud properties over satellite-observing geometry and solar illumination geometry.

It is worth emphasizing again that bidirectional reflectance differences between different cloud models result primarily from the differences in the first-order-scattering contribution to the reflection function R, i.e., from scattering phase function differences. In typical satellite observations, most illumination and reflection geometries correspond to side-scattering angles from about 50° to about 150°. Therefore the relatively small phase function differences at side-scattering angles between fractal and hexagonal ice particles (Figure 1) make the measured bidirectional reflectance patterns for the two cloud models rather similar, as computations depicted in Plate 2 show. In a practical test using the random-fractal and regular-hexagonal models in retrieving the optical thickness of ice clouds (3 days of global data from ISCCP), we found that global mean values of optical thickness were the same to within a few percent (and systematically lower than obtained using the water droplet model) but that individual values differed with an rms magnitude of about 20%. On the average, the use of the regular hexagonal rather than random-fractal model gives slightly larger values of the optical thickness. The only exceptions are the relatively narrow regions of forward and backscattering geometries where the pronounced halos and the strong backscattering peak in the hexagonal phase function cause significant reflection function differences between the two types of ice clouds (Plate 2). Such backscattering geometries are common in geostationary satellite images but occupy less than a few percent of the whole image. Interestingly, recent analyses of Polarization and Directionality of the Earth's Reflectances instrument (POLDER) bidirectional reflectance measurements of cirrus clouds (J. Descloitres, private communication, 1995) have shown that theoretical computations using regular hexagonal crystals significantly overestimate the measured backscattering reflectance, whereas computations exploiting the phase function for random fractals provide a good fit. This result is in full agreement with computations displayed in Plate 2 if one assumes that the cirrus clouds measured consisted predominantly of highly irregular ice particles rather than of perfect hexagonal crystals.

4. Conclusions

We have used the fractal-particle phase function as well as the phase function for projected-area-equivalent hexagonal crystals and the standard ISCCP water droplet model in detailed and numerically accurate computations of the albedo and bidirectional reflectivity for plane-parallel ice and water clouds at a nonabsorbing wavelength of 0.63 μm. Since our computations pertain to a visible wavelength at which ice absorption is negligible, all quantities that have been computed and analyzed are phase function dependent only and do not entail new ways of treating absorption by nonspherical particles [cf. *Mitchell and Arnott*, 1994]. Because of a smaller asymmetry parameter the global and planetary albedos of an ice cloud composed of regular hexagonal crystals are systematically higher than those of a liquid water cloud with the same optical thickness [cf. *Kinne and Liou*, 1989; *Minnis et al.*, 1993a; *Sun and Shine*, 1995]. The even smaller asymmetry parameter for fractal ice particles further increases the planetary and global albedos, making them substantially larger than those for optical-thickness-equivalent water clouds. These calculations demonstrate the importance of adequately modeling the shape (and/or internal structure) of ice particles in evaluating the impact of cirrus clouds on climate.

Given the nonspherical-spherical differences in the single-scattering phase functions, ice clouds are significantly brighter than liquid water clouds of the same optical thickness at most side-scattering geometries. This result is in agreement with the conclusion of *Minnis et al.* [1993a] and means that using the water droplet phase function in analyzing reflectance measurements for cirrus clouds, as done in the first version of the ISCCP, would often overestimate the cloud optical thickness. We have shown, however, that this is not universally true for all scattering geometries and that the larger planetary albedo of ice clouds does not always translate into larger bidirectional reflectivity. Specifically, at forward and backscattering azimuths a liquid water cloud can be substantially brighter than an optical-thickness-equivalent ice cloud composed of random-fractal crystals. At forward scattering geometries, this is also true for hexagonal-particle versus liquid-water clouds. We have shown that the use of the wrong particle model in retrieving the cloud optical thickness from bidirectional reflectance measurements can result in an underestimation or an overestimation of the actual optical thickness by a factor that can exceed 3. Moreover, in some cases the erroneous use of the ice particle model in retrieving the optical thickness of a water cloud can result in unphysically large values of the optical thickness or can give no solution at all. Thus our results further emphasize the importance of accurately modeling the phase function of cloud particles in analyzing remotely sensed bidirectional reflectance data.

Overall reflection function differences between fractal-particle and hexagonal-particle ice clouds are significantly

smaller than those between fractal-particle and liquid-water clouds except at back scattering azimuths where hexagonal-particle clouds can be noticeably brighter than optical-thickness-equivalent fractal-particle clouds. As we discussed in the introduction, there is experimental evidence that the phase function of a randomly shaped ice crystal better represents the single-scattering properties of most cirrus clouds than the regular hexagonal model. Therefore fractal-hexagonal reflection function differences should be explicitly taken into account if bidirectional reflectance data for the same pixel are taken at a wide range of scattering angles, e.g., by employing along-track scanning [e.g., *Diner et al.*, 1991; *Travis*, 1993; *Deschamps et al.*, 1994]. On the other hand, fractal-hexagonal reflectance differences at most side-scattering directions are especially small. Therefore as our practical test using ISCCP data shows, in analyzing AVHRR-type measurements both fractal-particle and hexagonal-particle phase functions can give results which are close to each other but are distinctly different from those obtained using the liquid water model.

Acknowledgments. We are grateful to P. Minnis for providing results of his computations and thank B. E. Carlson, P. Minnis, and L. D. Travis for many useful discussions, S. Kinne and D. L. Mitchell for constructive reviews, and N. T. Zakharova for help with graphics. This work was supported by the NASA FIRE III project.

References

Arnott, W. P., Y. Y. Dong, J. Hallett, and M. R. Poellot, Role of small ice crystals in radiative properties of cirrus: A case study, FIRE II, November 22, 1991, *J. Geophys. Res.*, *99*, 1371-1381, 1994.

Bohren, C. F., and S. B. Singham, Backscattering by nonspherical particles: A review of methods and suggested new approaches, *J. Geophys. Res.*, *96*, 5269-5277, 1991.

de Haan, J. F., P. B. Bosma, and J. W. Hovenier, The adding method for multiple scattering calculations of polarized light, *Astron. Astrophys.*, *183*, 371-391, 1987.

de Rooij, W. A., and C. C. A. H. van der Stap, Expansion of Mie scattering matrices in generalized spherical functions, *Astron. Astrophys.*, *131*, 237-248, 1984.

Deschamps, P.-Y., F.-M. Bréon, M. Leroy, A. Podaire, A. Bricaud, J.-C. Buriez, and G. Séze, The POLDER mission: Instrument characteristics and scientific objectives, *IEEE Trans. Geosci. Remote Sens.*, *32*, 598-615, 1994.

Diner, D. J., C. J. Bruegge, J. V. Martonchik, G. W. Bothwell, E. D. Danielson, E. L. Floyd, V. G. Ford, L. E. Hovland, K. L. Jones, and M. L. White, A multi-angle imaging spectroradiometer for terrestrial remote sensing from the Earth Observing System, *Int. J. Imaging Syst. Technol.*, *3*, 92-107, 1991.

Foot, J. S., Some observations of the optical properties of clouds, II, Cirrus, *Q. J. R. Meteorol. Soc.*, *114*, 145-164, 1988.

Francis, P. N., Some aircraft observations of the scattering properties of ice crystals, *J. Atmos. Sci.*, *52*, 1142-1154, 1995.

Francis, P. N., A. Jones, R. W. Saunders, K. P. Shine, A. Slingo, and Z. Sun, An observational and theoretical study of the radiative properties of cirrus: Some results from ICE'89, *Q. J. R. Meteorol. Soc.*, *120*, 809-848, 1994.

Fu, Q., and K. N. Liou, Parameterization of the radiative properties of cirrus clouds, *J. Atmos. Sci.*, *50*, 2008-2025, 1993.

Gayet, J.-F., O. Crépel, and J.-F. Fournol, A new polar nephelometer for in situ measurements of microphysical and optical properties of clouds, in *Proceedings of the Conference on Cloud Physics*, pp. 26-30, Am. Meteorol. Soc., Boston, Mass., 1995.

Hansen, J. E., Multiple scattering of polarized light in planetary atmospheres, II, Sunlight reflected by terrestrial water clouds, *J. Atmos. Sci.*, *28*, 1400-1426, 1971.

Hansen, J. E., and L. D. Travis, Light scattering in planetary atmospheres, *Space Sci. Rev.*, *16*, 527-610, 1974.

Iaquinta, J., H. Isaka, and P. Personne, Scattering phase function of bullet rosette ice crystals, *J. Atmos. Sci.*, *52*, 1401-1413, 1995.

Kinne, S, and K.-N. Liou, The effect of the nonsphericity and size distribution of ice crystals on the radiative properties of cirrus clouds, *Atmos. Res.*, *24*, 273-284, 1989.

Kinne, S., T. P. Ackerman, A. J. Heymsfield, F. P. J. Valero, K. Sassen, and J. D. Spinhirne, Cirrus microphysics and radiative transfer: Cloud field study on 28 October 1986, *Mon. Weather Rev.*, *120*, 661-684, 1992.

Kinne, S., R. Bergstrom, T. P. Ackerman, A. J. Heymsfield, J. DeLuisi, M. Shiobara, P. Pilewskie, F. P. J. Valero, and Y. Takano, Cirrus cloud solar radiative properties: Comparisons between theory and observation based measurements during FIRE'91, in *Eighth Conference on Atmospheric Radiation*, pp. 238-240, Am. Meteorol. Soc., Boston, Mass., 1994.

Lacis, A. A., and J. E. Hansen, A parameterization for the absorption of solar radiation in the earth's atmosphere, *J. Atmos. Sci.*, *31*, 118-133, 1974.

Macke, A., Scattering of light by polyhedral ice crystals, *Appl. Opt.*, *32*, 2780-2788, 1993.

Macke, A., Modeling of the optical properties of cirrus clouds, Ph.D. thesis, Hamburg Univ., Germany, 1994.

Macke, A., and M. I. Mishchenko, On the applicability of regular particle shapes in light scattering calculations for atmospheric ice particles, *Appl. Opt.*, *35*, in press, 1996.

Macke, A., J. Mueller, and E. Raschke, Single scattering properties of atmospheric ice crystals, *J. Atmos. Sci.*, in press, 1996.

Minnis, P., K.-N. Liou, and Y. Takano, Inference of cirrus cloud properties using satellite-observed visible and infrared radiances, I, Parameterization of radiance fields, *J. Atmos. Sci.*, *50*, 1279-1304, 1993a.

Minnis, P., P. W. Heck, and D. F. Young, Inference of cirrus cloud properties using satellite-observed visible and infrared radiances, II, Verification of theoretical cirrus radiative properties, *J. Atmos. Sci.*, *50*, 1305-1322, 1993b.

Mishchenko, M. I., The fast invariant imbedding method for polarized light: Computational aspects and numerical results for Rayleigh scattering, *J. Quant. Spectrosc. Radiat. Transfer*, *43*, 163-171, 1990.

Mishchenko, M. I., A. A. Lacis, B. E. Carlson, and L. D. Travis, Nonsphericity of dust-like tropospheric aerosols: Implications for aerosol remote sensing and climate modeling, *Geophys. Res. Lett.*, *22*, 1077-1080, 1995.

Mitchell, D. L., and W. P. Arnott, A model predicting the evolution of ice particle size spectra and radiative properties of cirrus clouds, II, Dependence of absorption and extinction on ice crystal morphology, *J. Atmos. Sci.*, *51*, 817-832, 1994.

Muinonen, K., K. Lumme, J. Peltoniemi, and W. M. Irvine, Light scattering by randomly oriented crystals, *Appl. Opt.*, *28*, 3051-3060, 1989.

Muinonen, K., T. Nousiainen, P. Fast, K. Lumme, and J. I.

Peltoniemi, Light scattering by Gaussian random particles: Ray optics approximation, *J. Quant. Spectrosc. Radiat. Transfer*, in press, 1996.

Peltoniemi, J. I., K. Lumme, K. Muinonen, and W. M. Irvine, Scattering of light by stochastically rough particles, *Appl. Opt.*, *28*, 4088-4095, 1989.

Posse, P., and W. von Hoyningen-Huene, Information about scattering properties and particle characteristics of a stratiform cloud at Helgoland by remote optical measurements, *Beitr. Phys. Atmos.*, *68*, 359-366, 1995.

Rossow, W. B., and R. A. Schiffer, ISCCP cloud data products, *Bull. Am. Meteorol. Soc.*, *72*, 2-20, 1991.

Rossow, W. B., A. W. Walker, D. E. Beuschel, and M. D. Roiter, International Satellite Cloud Climatology Project (ISCCP), Documentation of New Cloud Dataset, *WMO/TD 737*, 115 pp., World Clim. Res. Programme, World Meteorol. Organ., Geneva, 1996.

Sassen, K., and K.-N. Liou, Scattering of polarized laser light by water droplet, mixed-phase and ice-crystal clouds, I, Angular scattering patterns, *J. Atmos. Sci.*, *36*, 838-851, 1979.

Sassen, K., N. C. Knight, Y. Takano, and A. J. Heymsfield, Effects of ice-crystal structure on halo formation: Cirrus cloud experimental and ray-tracing modeling studies, *Appl. Opt.*, *33*, 4590-4601, 1994.

Sato, M., K. Kawabata, and J. E. Hansen, A fast invariant imbedding method for multiple scattering calculations and an application to equivalent widths of CO_2 lines on Venus, *Astrophys. J.*, *216*, 947-962, 1977.

Stackhouse, P. W., Jr., and G. L. Stephens, A theoretical and observational study of the radiative properties of cirrus: Results from FIRE 1986, *J. Atmos. Sci.*, *48*, 2044-2059, 1991.

Stephens, G. L., S.-I. Tsay, P. W. Stackhouse, and P. J. Flatau, The relevance of the microphysical and radiative properties of cirrus clouds to climate and climatic feedback, *J. Atmos. Sci.*, *47*, 1742-1753, 1990.

Sun, Z., and K. P. Shine, Parameterization of ice cloud radiative properties and its application to the potential climatic importance of mixed-phase clouds, *J. Clim.*, *8*, 1874-1888, 1995.

Takano, Y., and K. N. Liou, Solar radiative transfer in cirrus clouds, I, Single-scattering and optical properties of hexagonal ice crystals, *J. Atmos. Sci.*, *46*, 3-19, 1989.

Travis, L. D., Earth observing scanning polarimeter, in *Long-Term Monitoring of Global Climate Forcings and Feedbacks*, edited by J. Hansen, W. Rossow, and I. Fung, *NASA Conf. Publ. 3234*, pp. 40-46, 1993.

van de Hulst, H. C., *Multiple Light Scattering*, 739 pp., Academic Press, San Diego, Calif., 1980.

Volkovitskiy, O. A., L. N. Pavlova, and A. G. Petrushin, Scattering of light by ice crystals, *Izv. Russ. Acad. Sci. Atmos. Ocean. Phys.*, *16*, 98-101, 1980.

Warren, S. G., Optical constants of ice from the ultraviolet to the microwave, *Appl. Opt.*, *23*, 1206-1225, 1984.

Wielicki, B. A., J. T. Suttles, A. J. Heymsfield, R. M. Welch, J. D. Spinherne, M.-L. Wu, D. O'C. Starr, L. Parker, and R. F. Arduini, The 27-28 October 1986 FIRE IFO cirrus case study: Comparison of radiative transfer theory with observations by satellite and aircraft, *Mon. Weather Rev.*, *118*, 2356-2376, 1990.

Wiscombe, W. J., On initialization, error and flux conservation in the doubling method, *J. Quant. Spectrosc. Radiat. Transfer*, *16*, 637-658, 1976.

Zhang, J., and L. Xu, Light scattering by absorbing hexagonal ice crystals in cirrus clouds, *Appl. Opt.*, *34*, 5867-5874, 1995.

A. A. Lacis and W. B. Rossow, NASA Goddard Institute for Space Studies, 2880 Broadway, New York, NY 10025. (e-mail: ccaal@giss.nasa.gov and clwbr@giss.nasa.gov)

A. Macke, Columbia University and NASA Goddard Institute for Space Studies, 2880 Broadway, New York, NY 10025. (e-mail: craxm@giss.nasa.gov)

M. I. Mishchenko (corresponding author), NASA Goddard Institute for Space Studies, 2880 Broadway, New York, NY 10025. (e-mail: crmim@giss.nasa.gov)

(Received December 5, 1995; revised March 27, 1996, accepted March 27, 1996.)